Journal of Geriatric Cardiology (2017) 14: 292–300

Research Article · Open Access ·

Expression of p53 in myocardium following coronary microembolization in rats and its significance

Yu-Han SUN, Qiang SU, Lang LI, Xian-Tao WANG, Yuan-Xi LU, Jia-Bao LIANG

Department of Cardiology, the First Affiliated Hospital of Guangxi Medical University, Nanning, China

Abstract

Background Cardiomyocyte apoptosis is a primary cause for coronary microembolization (CME)-induced cardiac dysfunction. p53 induces cell growth retardation and apoptosis through stress pathway. The present study investigated the mechanism of p53-induced myocardial apoptosis and cardiac dysfunction by activating the mitochondrion apoptotic pathway following CME. **Methods** Forty SD rats were equally divided into microembolization (CME), sham operation (sham), CME+siRNA-p53, and CME+control-p53 groups. The CME rat model was established by injecting microembolization spheres via the left ventricle. Cardiac ultrasound, TUNEL, fluorescence quantitative PCR, and Western blot were used to assess the cardiac function indicators, cardiomyocyte apoptosis, and the expressions of mRNA and protein in myocardial tissues, respectively. **Results** Echocardiography revealed a significantly reduced cardiac function of the CME group than the sham group while the CME-induced cardiac dysfunction was improved in the CME+siRNA-p53 group. The indicators of myocardial apoptosis in the CME group increased significantly than the sham group; those of the CME+siRNA-p53 group decreased significantly than the CME group. Fluorescence quantitative PCR and Western blot demonstrated that p53, Bbc3 (PUMA), and cleaved caspase-3 expressions were significantly increased, and BCL-2 expression was declined in myocardial tissues of the CME group compared to the sham group. A contrasting result was observed in the CME+siRNA-p53 group as compared to the CME group. **Conclusions** P53 is involved in the CME-induced cardiac dysfunction, which may up-regulate Bbc3 to activate BCL-2/caspase3 mitochondrial apoptotic pathway and induce myocardial apoptosis. Inhibiting the p53 expression can effectively suppress this pathway, thereby reducing myocardial apoptosis and cardiac dysfunction.

J Geriatr Cardiol 2017; 14: 292–300. doi:10.11909/j.issn.1671-5411.2017.05.007

Keywords: Bbc3; BCL-2; Cardiac dysfunction; Coronary microembolization; Myocardial apoptosis; p53

1 Introduction

Coronary microembolization (CME) is a coronary microcirculation embolism and myocardial microinfarction caused by spontaneous rupture of coronary atherosclerotic plaques or microemboli during percutaneous coronary intervention (PCI).[1] The incidence of CME during perioperative PCI has been reported as 15%–20% and is up to 45% in high-risk patients.[2] CME may lead to postoperative "no-flow" or "slow-flow" as well as microcirculation dysfunction, subsequently resulting in myocardial ischemia, arrhythmia, heart failure, and other consequences and is a strong predictor for the long-term major adverse cardiovascular events.[3,4]

Studies have revealed that CME can stimulate the cardiomyocyte apoptosis and inflammation in local myocardial tissues, and thus speculate that apoptosis and inflammation are the two major pathological mechanisms of progressive cardiac function deterioration following CME.[5,6] Our previous studies found prominent myocardial cells apoptosis in the infarction-related regions after CME. On the other hand, the expression of apoptosis-related proteins, the caspase family, was significantly increased and the expression of the apoptosis-related protein BCL-2 family was altered. These phenomena proved that both the mitochondrial apoptosis pathway and death receptor pathway are involved in the CME-induced myocardial injury process.[2,5] p53 is a critical apoptosis-related gene and participates in apoptosis initiation, which can regulate the process through the death receptor pathway, Bax/BCL2, NF receptor, Fas protein, and other pathways.[7] Jiang, *et al*.,[8] found that p53 expression in myocardial tissues was upregulated during myocardial ischemia-reperfusion (I/R), and was positively correlated with the myocardial apoptosis level. Xiao, *et al*.,[9] revealed

Correspondence to: Lang Li, MD, Department of Cardiology, the First Affiliated Hospital of Guangxi Medical University, No. 6 Shuangyong road, Nanning 530021, China. E-mail: drlilang@163.com

Telephone: +86-0771-5359801 **Fax:** +86-0771-5331171

Received: April 4, 2017 **Revised:** May 3, 2017

Accepted: May 21, 2017 **Published online:** May 28, 2017

that the cardiomyocyte apoptosis was reduced after mitochondrial apoptotic pathway was inhibited; the p53 expression was also down-regulated. Some studies reported that the down-regulation of p53 expression could reduce myocardial apoptosis during myocardial infarction.[10,11] In our previous studies, p53 expression was found to be up-regulated in CME rats using gene expression profile microarray. Nevertheless, whether p53 activates the mitochondrial apoptotic pathway during CME, and whether it is possible to modulate the CME-induced myocardial apoptosis by p53 interference is yet unclear.

Therefore, the present study aimed to evaluate the p53 expression and its correlation with the mitochondrial pathway in CME rats. We also performed interference of p53 expression to reveal its role in CME-induced cardiac dysfunction and cardiomyocyte apoptosis.

2 Methods

2.1 CME modeling and experimental grouping

The present study was approved by the Ethics Committee of Guangxi Medical University and implemented in accordance with the animal experiment management practice. In addition, the treatment and usage of laboratory animals were in accordance with National Institute of Health (NIH Publication No. 85–23, revised in 1996).

Forty SD rats (aged 8 weeks, weight 250–300g, male or female, provided by the Laboratory Animal Center, Guangxi Medical University) were randomly assigned to 4 groups (n = 10 in each group): CME group, sham group, CME+siRNA-P53 group, and CME+control-p53 group.

CME modeling: rats of the CME+siRNA-p53 and CME+control-p53 groups were treated as described previously by Mao, *et al*.,[12] wherein the adeno-associated virus subtype 9 (AAV9, GeneChem, China) was considered as the vector carrying the p53-siRNA sequences (5′-CACCTAATTCC ATGGAAGATCTGTT-3′) and control-siRNA sequences (5′-TTCTCCGAACGTGTCACGT-3′), respectively, for transduction. Then, the virus carrying the p53-siRNA and control-siRNA sequences was injected into different rats via the tail vein on day 14 prior to CME modeling—1×10^{11} TU/animal. Rats were injected with propofol via the tail vein for anesthesia, followed by endotracheal intubation and connection to the ventilator. Then, the chest was opened along the left margin of the sternum, and the pericardium was stripped. Subsequently, 4000 U polystyrene microspheres were injected via the left ventricle [microspheres were suspended in 0.1 mL normal saline containing sodium dodecyl sulfate (SDS), and the ascending aorta was clamped for 20 cardiac cycles (10 s)]. The chest was closed, and rats were injected with 10000 U penicillin through the tail vein. After the animals recovered from anesthesia, they were housed in a clean environment for 8 h before specimens were collected. Eight hours after CME was chosen because of the peak cardiac dysfunction in our preliminary experiments and previous studies.[13] The animals in the sham group received 0.1 mL normal saline using similar procedures.

2.2 Evaluation of transduction efficiency

AAV9 vector (GeneChem, China) carrying p53-siRNA and control-siRNA fluorescent-labelled fragments were prepared. For rats in the CME+siRNA-p53 group, the left ventricle tissue was collected from the frozen section at 14 days after transduction and observed under a fluorescence microscope (magnification 100 ×) to assess the transduction efficiency. Image Pro Plus 6.0 (Media Cybernetics, USA) was used to analyze the fluorescence image, and the rate of transduction was estimated by comparing the fluorescence area with the total tissue area.

2.3 Detection of cardiac function in rats

The cardiac function was detected using Philips Sonos 7500 cardiovascular ultrasound machine at 8 h after CME, wherein the transducer frequency of 12 MHz was selected and the following parameters in each rat were measured: left ventricular ejection fraction (LVEF), left ventricular end diastolic diameter (LVEDd), left ventricular fractional shortening (FS), and cardiac output (CO). All the estimations were averaged over three cardiac cycles. All the echocardiographic examinations were performed by a specialist with extensive echocardiographic experience.

2.4 Detection of cardiomyocyte apoptosis by TUNEL assay

The left ventricle was harvested from CME rats for paraffin sections, which were evaluated using the TUNEL Assay kit (Roche, USA). Under a fluorescence microscope, 5 high-power fields (magnification 100 ×) were randomly selected and imaged. The TUNEL-positive signals were located in the nuclei, and the apoptotic nuclei in the myocardial sections exhibited green fluorescence. Image Pro Plus 6.0 (Media Cybernetics, USA) was used to count the fluorescently stained nuclei (TUNEL and DAPI). The cardiomyocyte apoptosis indicator = number of apoptotic cardiomyocytes/total number of cardiomyocytes × 100%.

2.5 Western blot assay

Total protein extracted using the total protein extraction kit for cells and tissues (KangChen KC-415, China), was estimated using the BCA protein quantitation kit (Kang-

Chen KC-430). Subsequently, 50 μg protein sample per lane was resolved on the SDS-PAGE and transferred to polyvinylidene fluoride membranes (Millipore, USA), followed by incubation in 5% BSA at room temperature for 1 h to block the non-specific binding. Then, the membrane was probed with the respective primary antibodies: mouse anti-rat p53 mAb (No. #2524), rabbit anti-rat polyclonal antibody (No. #7467), rabbit anti-rat BCL-2 polyclonal antibody (No. #2876), and rabbit anti-rat mAb (No. #14220) (all from Cell Signaling Technology, USA, 1: 1000), overnight at 4°C. GAPDH (KangChen, 1: 10000) served as the internal reference. The membranes were washed with TBST, followed by addition of horseradish peroxidase-labeled secondary antibody (KangChen, 1: 5000), incubated at room temperature for 1 h. Finally, the immunoreactive bands were developed with enhanced chemiluminescence (ECL) and exposed to X-ray films (TianNeng, China). The gray-scale intensity of the bands was analyzed using the ImageJ software.

2.6 Fluorescence quantitative PCR analysis

Total RNA was extracted from the left ventricular myocardium, using TRIzol (Invitrogen, USA), according to the manufacturer's instructions and quantified using NanoDrop (Thermo Fisher Scientific, USA). Reverse transcription was performed using cDNA reverse transcription kit (Takara, Japan). Relative quantification was performed using the $2^{-\Delta\Delta CT}$ method, in which the β-actin served as the internal reference. Amplification system used ABI StepOne system (Applied BioSystems, USA). The primer sequences synthesized were as follows: p53 forward 5′-TCCTCCCCAA CATCTTATCC-3′, reverse 5′-GCACAAACACGAACCT CAAA-3′, Bbc3 forward 5′-ACTGCCAGCCTTGCTTGT C-3′, reverse 5′-AGTCCTTCAGCCCTCCCTTC-3′, BCL-2 forward 5′-GACTGAGTACCTGAACCGGCATC-3′, reverse 5′-CTAGACAGCGTCTTCAGAGACA-3′, β-actin forward 5′-GGAGATTACTGCCCTGGCTCCTA-3′, reverse 5′-GA CTCATCGTACTCCTGCTTGCTG-3′.

2.7 Statistical analysis

Data were analyzed using SPSS 23.0 software (IBM Corporation, Chicago, USA). Measurement data were expressed as mean ± SD. The two groups were compared using *t*-test, whereas multi-group comparisons were carried out using one-way ANOVA. The multiple comparisons among groups were performed using the LSD test. A difference with $P < 0.05$ was considered statistically significant.

3 Results

3.1 AAV9 transduction rate of myocardium in rats

In the pre-trial, we found that AAV9 with fluorescent fragments showed the highest efficiency after it was transfected in rats for 14 days. Herein, we selected the frozen sections of myocardium that were transfected for 14 days and observed under a fluorescence microscope (magnification 100×), which showed a transduction rate of 43.09% ± 7.98% (Figure 1).

3.2 Alteration of cardiac function indicators in rats

LVEF, FS, CO, and LVEDD values were determined using echocardiography, which were used to evaluate the cardiac function in rats. The results at 8 h after CME modeling (Table 1) revealed that: (1) compared to the sham group, the cardiac function was significantly decreased in the CME and CME+control-p53 groups, which manifested as myocardial contractile dysfunction and left ventricle dilatation, such as declined LVEF, FS, and CO ($P < 0.05$), as well as, increased LVEDD ($P < 0.05$). (2) Compared to the CME group, the CME-induced cardiac dysfunction was improved in the CME+siRNA-p53 group, manifesting as high LVEF, FS, and CO ($P < 0.05$), as well as decreased LVEDD ($P < 0.05$).

3.3 Observation of cardiomyocyte apoptosis in rats

Apoptotic nuclei were stained with green fluorescence (Figure 2A). The cardiomyocyte apoptosis was occasionally found under the endocardium in the sham group. The cardiomyocyte apoptosis indicators of the CME, sham, CME+ siRNA-p53, and CME+control-p53 groups were 10.163% ± 1.71%, 0.63% ± 0.34%, 5.63% ± 1.10%, and 10.63% ± 1.59%, respectively (Figure 2B). Notably, the cardiomyocyte apoptosis indicator was significantly higher in the CME and CME+control-p53 groups as compared to the sham group ($P < 0.05$), and lower in the CME+ siRNA- p53 group as compared to the CME group ($P < 0.05$).

3.4 Comparison of p53, Bbc3, and BCL-2 mRNA expressions (Figures 3)

Compared to the sham group, p53 and Bbc3 mRNA expressions in the cardiomyocytes of the CME and CME+ control-p53 groups were significantly increased ($P < 0.05$), whereas the BCL-2 mRNA expression was significantly decreased ($P < 0.05$). Compared to the CME group, p53 and Bbc3 mRNA expressions of the CME+siRNA-p53 group were significantly lower ($P < 0.05$), whereas the BCL-2 mRNA expression was significantly increased ($P < 0.05$).

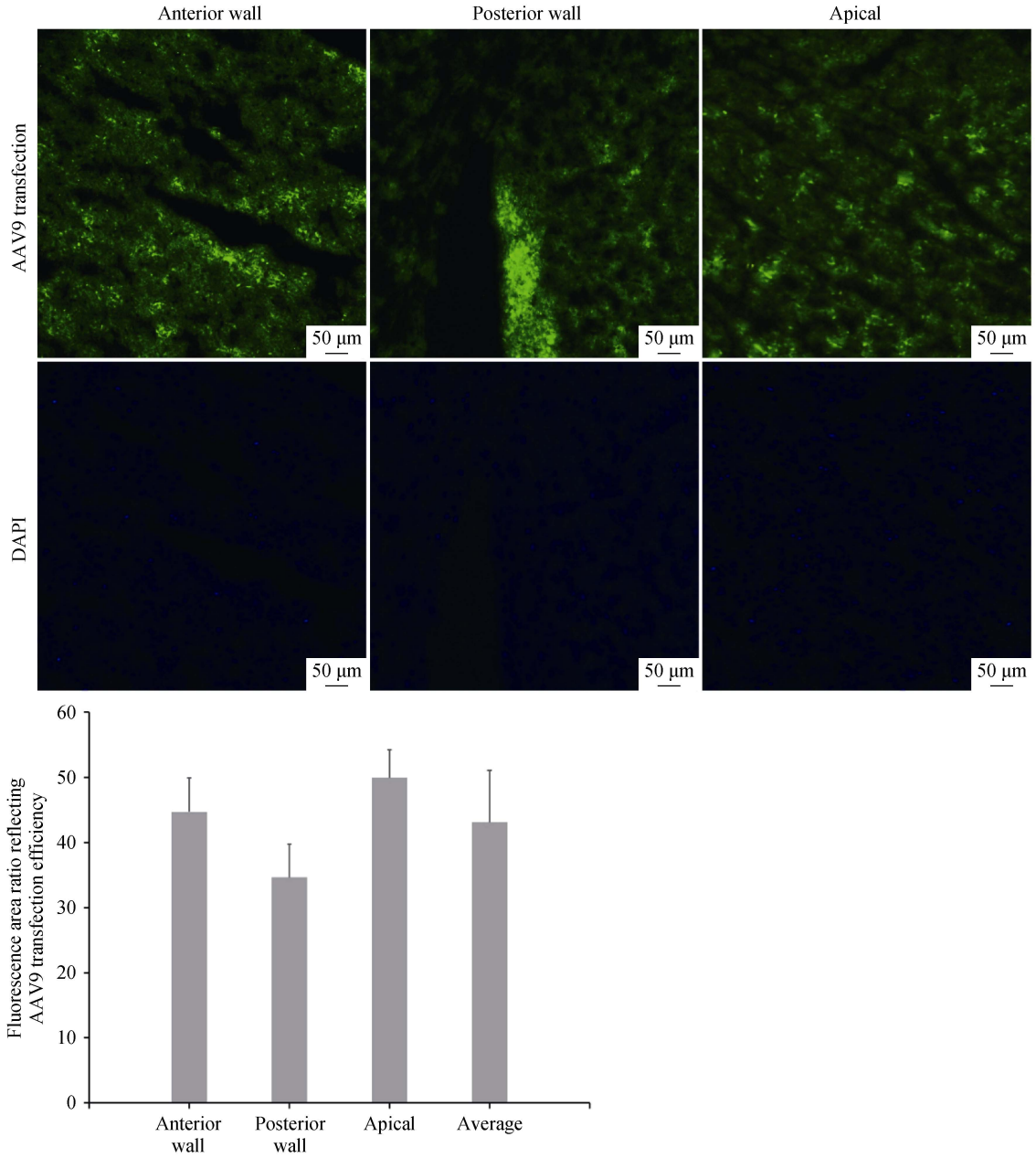

Figure 1. Fluorescence area ratio reflecting the AAV9 transduction efficiency in different locations of the ventricle of myocardial tissues under a fluorescence microscope. Anterior wall: 44.71% ± 5.23%, posterior wall: 34.64% ± 5.07%, apical: 49.94% ± 4.3%, average: 43.09% ± 7.98%. All scale bars represent 50 μm (magnification 100 ×).

Table 1. Changes in cardiac function indicators in rats from various groups.

	N	LVEF, %	FS, %	CO, L/min	LVEDD, mm
CME group	10	35.77 ± 2.63$^{\#}$	0.15 ± 0.01$^{\#}$	0.12 ± 0.01$^{\#}$	0.81 ± 0.06$^{\#}$
Sham group	10	88.73 ± 1.22	0.54 ± 0.02	0.23 ± 0.03	0.52 ± 0.04
CME+siRNA-p53 group	10	53.37 ± 2.51$^{*,\#}$	0.24 ± 0.02$^{*,\#}$	0.16 ± 0.02$^{*,\#}$	0.68 ± 0.06$^{*,\#}$
CME+control-p53 group	10	37.43 ± 0.95$^{\#}$	0.16 ± 0.01$^{\#}$	0.11 ± 0.01$^{\#}$	0.87 ± 0.04$^{\#}$

$^{*}P < 0.05$ compared with the CME group; $^{\#}P < 0.05$ compared with the sham group. CO: cardiac output; FS: left ventricular fractional shortening; LVEDD: left ventricular end diastolic diameter; LVEF: left ventricular ejection fraction; LVFS: left ventricular fractional shortening.

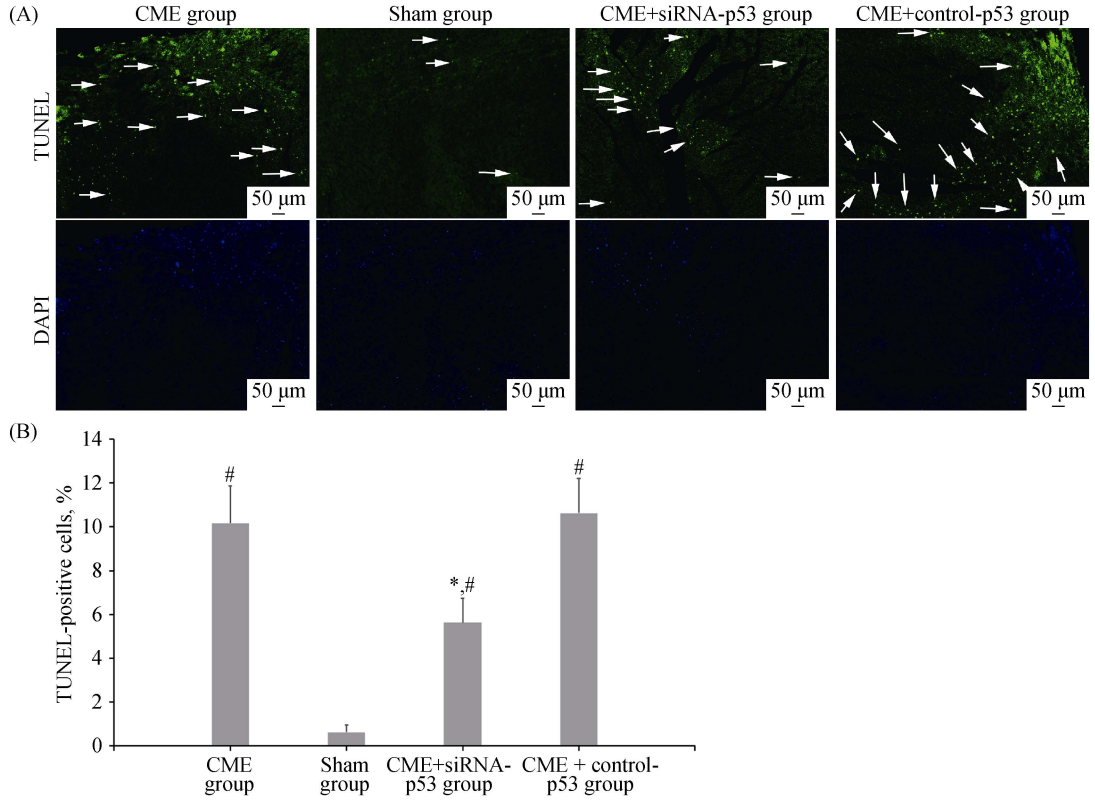

Figure 2. TUNEL staining of myocardial tissues. (A): Apoptotic nuclei emit green fluorescence; the arrows indicate apoptotic cardiomyocyte nuclei; (B): TUNEL-positive cell percent. $^{*}P < 0.05$ compared to the CME group; $^{\#}P < 0.05$ compared to the sham group. All scale bars represent 50 μm (magnification 100 ×). CME: coronary micro-embolization.

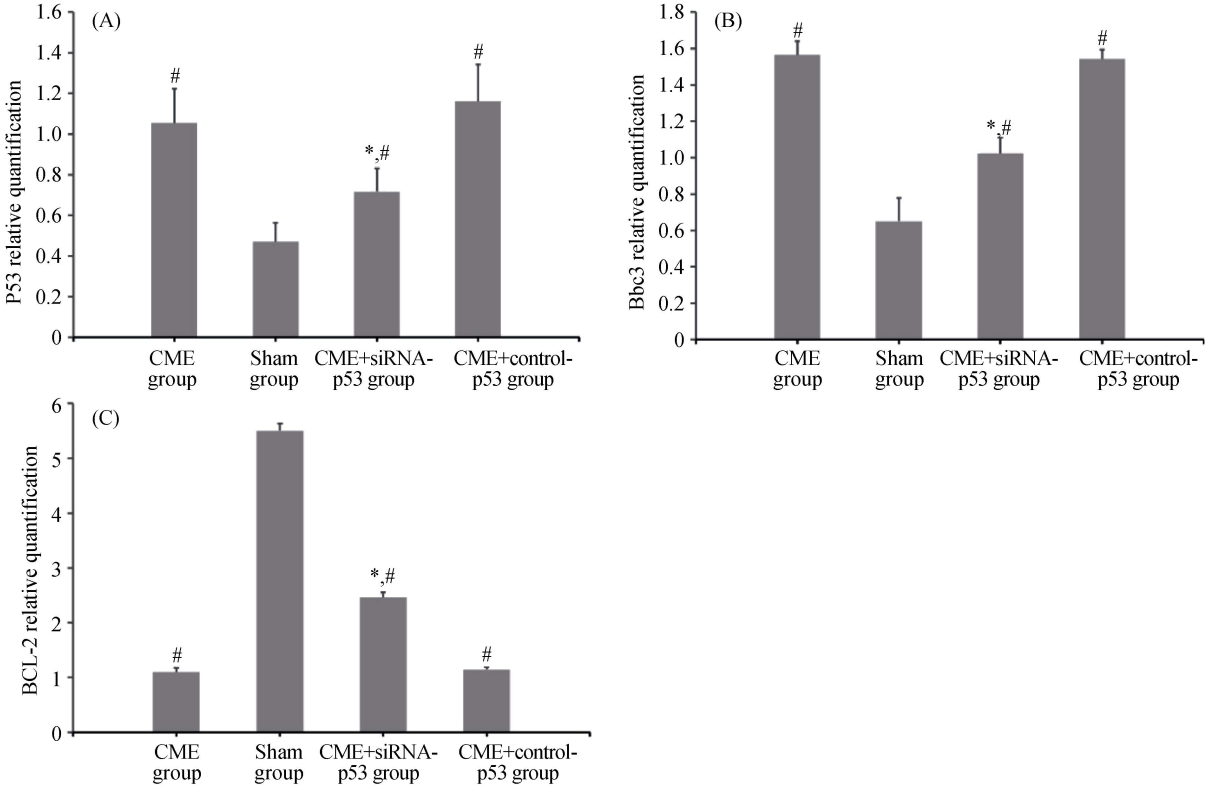

Figure 3. Fluorescence quantitative PCR results of p53 mRNA (A), Bbc3 mRNA (B) and BCL-2 mRNA (C) expressions in the four groups. $^{*}P < 0.05$ compared to the CME group, $^{\#}P < 0.05$ compared to the sham group. CME: coronary microembolization.

3.5 Detection of p53, Bbc3, BCL-2, and caspase-3 expression levels using Western blot assay (Figure 4)

Compared to the sham group, the relative expressions of p53, Bbc3, and cleaved caspase-3 in cardiomyocytes were significantly increased in the CME and CME+control-p53 groups ($P < 0.05$), while that of BCL-2 was significantly declined ($P < 0.05$). Compared to the CME group, the relative expressions of p53, Bbc3, and cleaved caspase-3 were significantly lower in the CME+siRNA-p53 group ($P < 0.05$), while that of BCL-2 was significantly increased ($P < 0.05$).

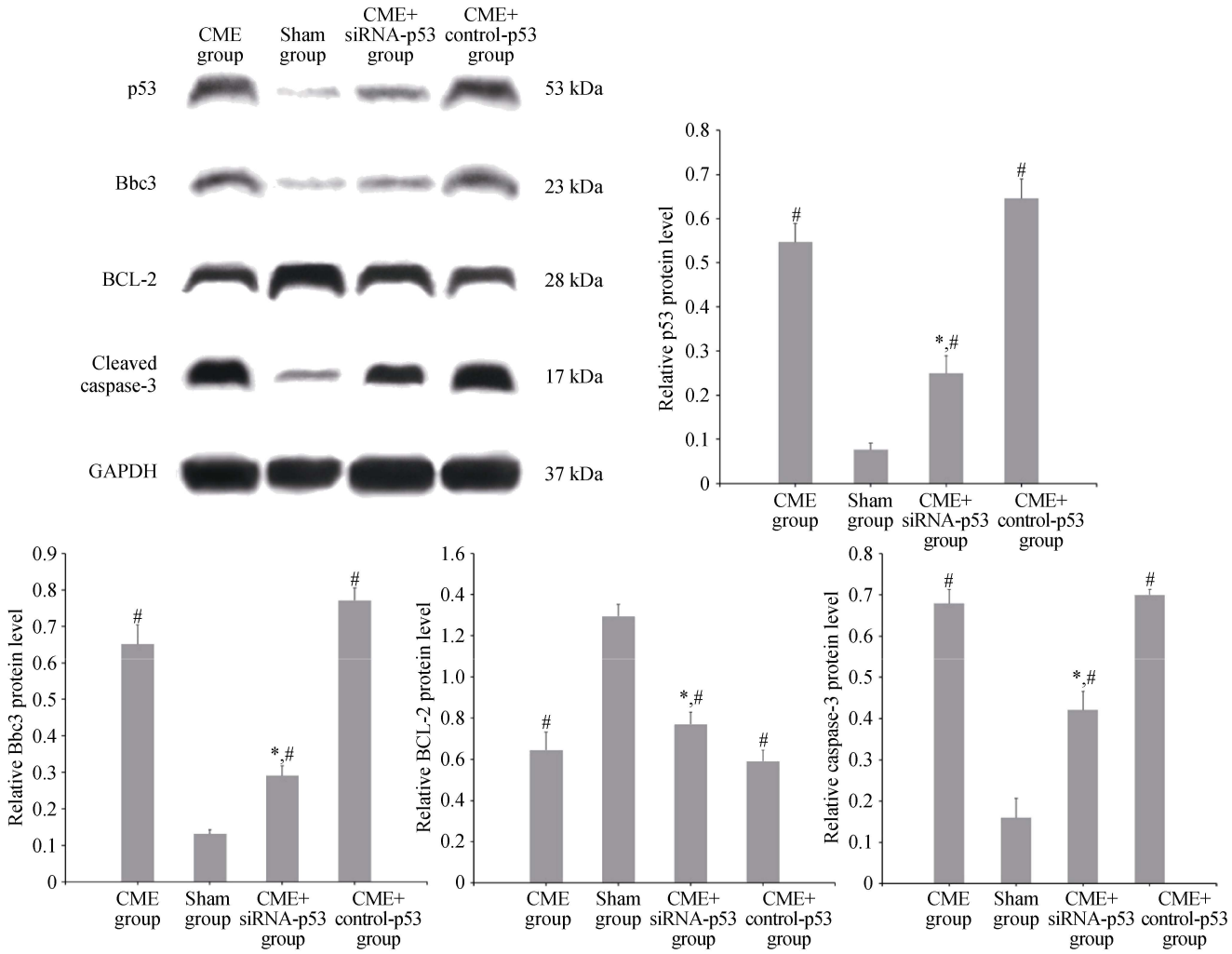

Figure 4. Western blot results of p53, Bbc3, BCL-2, and cleaved caspase-3 expressions in the four groups. *$P < 0.05$ compared to the CME group; #$P < 0.05$ compared to the sham group. CME: coronary micro-embolization.

3.6 Correlations among p53, Bbc3, BCL-2, cleaved caspase-3, and LVEF in cardiomyocytes of CME rats

In cardiomyocytes of CME rats, the p53 expression was significantly positively correlated with Bbc3 expression ($r = 0.828$, $P = 0.002$), positively correlated with cleaved caspase-3 expression ($r = 0.677$, $P = 0.033$), and negatively correlated with LVEF expression ($r = –0.880$, $P = 0.003$). On the other hand, the Bbc3 expression was negatively correlated with BCL-2 expression ($r = –0.733$, $P = 0.019$) and the cleaved caspase-3 expression was negatively correlated with LVEF expression ($r = –0.741$, $P = 0.003$).

4 Discussion

CME is a common complication during the plaque rupture in acute coronary syndrome and PCI. The condition can induce no-flow or slow-flow, and severely affect the cardiac function and long-term prognosis of the patients. This clinical issue is a major concern necessitating immediate attention.[3] Animal experiments have found regional minor myocardial infarction, myocardial necrosis, and apoptosis, as well as, progressive declined cardiac function in acute period of CME.[14] Gao, *et al*.,[15] observed that Bax, cyto-

chrome C, and cleaved caspase-3 expressions were increased and BCL-2 expression was decreased during myocardial I/R, thereby resulting in increased cardiomyocyte apoptosis. This indicated that the mitochondrial apoptotic pathway is involved in myocardial apoptosis. BCL-2 family, including anti-apoptotic BCL-2 protein and pro-apoptotic Bax protein, is an essential regulator of mitochondria-mediated apoptotic signaling pathways. Moreover, caspase-3 is the final step in the activation of apoptosis, and the activated products may act as markers of apoptosis.[16] In this study, we found that the myocardial apoptosis indicators were significantly increased following CME, the cleaved caspase-3 expression was significantly elevated, and the cardiac function was significantly declined. Notably, our data showed that at 8 h after CME, multiple micro-infarction foci appeared in the myocardium, myocardial apoptosis increased and the cardiac function decreased. In addition, compared to CME group, the myocardial apoptosis was significantly reduced in CME+siRNA-p53 group, and cardiac function was also significantly improved, this could be further confirmed that myocardial apoptosis was one of the main mechanisms of early cardiac dysfunction in CME, and cardiac dysfunction could be effectively improved by inhibiting apoptosis.

We also found that p53 expression in myocardial tissues was significantly increased indicating a significantly positive correlation with cleaved caspase-3 expression following CME, suggesting that p53 was likely to be involved in the process of myocardial apoptosis following CME. Initially found as a tumor suppressor gene, the role of p53 in the regulation of apoptosis has been gradually revealed in several subsequent studies. Su, *et al*.,[17] found that p53 mediated the NOXA expression during high glucose induced cardiomyocytes apoptosis, and revealed a novel regulatory mechanism of ROCK1/p53/NOXA signaling in modulating cardiomyocyte apoptosis *in vitro*. Hong, *et al*.,[18] reported that p53 acted upstream of SDF-1, which showed a cardioprotective effect in acute myocardial infarction. Zhang, *et al*.,[11] reported p53-inhibition reduced cardiomyocyte apoptosis through the target-PFTa. Nakamura, *et al*.,[19] found that p53 and its downstream cytochrome C oxidase 2 (SCO_2) protein were important regulators of mitochondrial respiration, p53/SCO_2 up-regulation increased the oxygen consumption of mitochondria, leading to the cardiac dysfunction associated with mitochondrial-derived ROS and lipid accumulation. Moreover, p53 can regulate the apoptosis through the regulation of its effector molecule, Bbc3 (p53 upregulated modulator of apoptosis, PUMA), on the mitochondrial apoptosis pathway.[7,20] Bbc3, a newly discovered BH3-only member of the Bcl-2 family, plays a critical role in p53-dependent and p53-independent apoptosis, wherein its interactions with BCL-2 and Bax might alter the permeability of the mitochondrial membrane.[21,22] Tu, *et al*.,[23] revealed that inhibiting the Bbc3 expression in cardiomyocytes could upregulate the BCL-2 level and reduce apoptosis, thereby playing a protective role on the myocardium. In addition, Gao, *et al*.,[24] found that Bbc3 expression in the myocardium was significantly reduced, thus the cardiomyocyte apoptosis was significantly decreased in mice receiving anti-Bbc3 treatment during myocardial I/R. These results postulate that Bbc3 can affect the cardiomyocyte apoptosis by regulating the BCL-2 level. In the current study, we found that the Bbc3 expression level was significantly elevated and BCL-2 was significantly declined in the myocardial tissues of CME rats, with a significantly negative correlation. Furthermore, pro-caspase-3 was trimmed into a large number of cleaved fragments, indicating that the BCL-2-dependent mitochondrial apoptotic pathway was activated, which was accompanied by cardiac function deterioration.

In order to further substantiate the relationship of p53 and Bbc3 with the mitochondrial apoptotic pathway, rats were administered with adeno-associated virus injection carrying p53-siRNA sequence via the tail vein at 14 days prior to CME modeling. The results showed that the p53 expression in myocardial tissues was significantly reduced following CME, and the myocardial apoptosis indicators, as well as cleaved caspase-3, were significantly decreased; thus, the cardiac function was noticeably improved as compared to the CME group. This confirmed our speculation that p53 is involved in the myocardial apoptosis process following CME, thereby causing CME-induced cardiac dysfunction. Simultaneously, we found that when the p53 level in the myocardium was downregulated, its effector molecule Bbc3 was inhibited. Conversely, the BCL-2 expression was significantly increased, which indicated that p53/Bbc3/BCL-2 signal transduction pathway plays a major role in CME-induced cardiac dysfunction. These characteristics suggested that blocking the p53 signaling pathway can inhibit the Bbc3 expression, reduce the activation of BCL-2-related mitochondrial apoptosis pathway, and thus, improve the cardiac dysfunction following CME.

The heart was rich in mitochondria that helped provide the energy required for optimal myocardial function. Mitochondria played a central role in cellular metabolism, Ca^{2+} handling and energy production, and mitochondrial-related apoptotic pathways played a key role in myocardial apoptosis.[25] Translocation of Bax to mitochondria and release of cytochrome were considered as the major mechanism of mitochondrial apoptosis pathway, leading to apoptosis.[26]

Our results and other studies demonstrated that overexpression of Bbc3 could activate mitochondrial apoptotic pathway via the BCL-2 family of apoptotic proteins and resulted in cardiomyocyte apoptosis.[21,22] Meanwhile, in our *in vivo* model, when the mitochondrial pathway was activated in CME group, the rats not only promoted myocardial apoptosis, but also exhibited cardiac dysfunction (abnormal LVEF and FS). Furthermore, when p53 expression was down-regulated by p53-siRNA, mitochondrial apoptotic pathway was inhibited, myocardial apoptosis was significantly reduced, and cardiac function was improved. These signs suggested that lost vitality due to mitochondrial apoptosis pathway was considered to be an important determinant in cardiac dysfunction. It was noteworthy that although we significantly reduced the expression level of p53/Bbc3, rats in CME+siRNA-p53 group still showed a lower BCL-2 expression than the sham group. After all, in addition to p53/Bbc3, the mitochondrial pathway was also regulated by other upstream factors. Luo, *et al*.,[27] reported that p38β could interfere with mitochondrial pathway by manganese superoxide dismutase. Wang, *et al*.,[28] found Omi/HtrA2 participated in mitochondrial-induced myocardial apoptosis. Also, ATP, calcium, Bax and other factors were reported to affect the mitochondrial apoptosis pathway.[25] And in our study, it could be seen that inhibiting BCL-2-related mitochondrial pathways by down-regulating p53/Bbc3 was an effective way to reduce myocardial apoptosis and cardiac dysfunction in CME.

The limitation of this study was that plastic microspheres were considered the micro-embolization agent in CME modeling, which varied from the embolic materials with bioactivity comprising of abundant platelets, red blood cells, and other substances that were generated by actual rupture of the coronary atherosclerotic plaques. And due to the limited rate of AAV9 myocardial transduction efficiency, P53 could not be completely silent. These might result in pathophysiological changes different from the real changes of CME caused by the plaque rupture.

In summary, p53 is involved in the myocardial apoptotic process arising from CME and plays a vital role in CME-induced cardiac function injury through the regulation of Bbc3/BCL-2 signal transduction pathway. Intervening p53 expression in myocardial tissues can effectively reduce the mitochondrial pathway-induced myocardial apoptosis and CME-induced cardiac dysfunction.

Acknowledgements

This study was supported by the grants from the National Natural Science Foundation of China (Grant No. 81260042) and Guangxi Natural Science Foundation (Grant No. 2016GXNSFBA380022).

References

1 Heusch G, Kleinbongard P, Bose D, *et al*. Coronary microembolization: from bedside to bench and back to bedside. *Circulation* 2009; 120: 1822–1836.
2 Li L, Su Q, Wang Y, *et al*. Effect of atorvastatin (Lipitor) on myocardial apoptosis and caspase-8 activation following coronary microembolization. *Cell Biochem Biophys* 2011; 61: 399–406.
3 Gong X, Yu J, Mao Y, Hu D. Anticoagulant therapy for non-ST-segment elevation acute coronary syndrome in China: A multicenter observational study. *J Transl Intern Med* 2014; 4: 25–28.
4 Carlsson M, Martin AJ, Ursell PC, *et al*. Magnetic resonance imaging quantification of left ventricular dysfunction following coronary microembolization. *Magn Reson Med* 2009; 61: 595–602.
5 Su Q, Li L, Liu YC, *et al*. Effect of metoprolol on myocardial apoptosis and caspase-9 activation after coronary microembolization in rats. *Exp Clin Cardiol* 2013; 18: 161–165.
6 Li L, Li DH, Qu N, *et al*. The role of ERK1/2 signaling pathway in coronary microembolization-induced rat myocardial inflammation and injury. *Cardiology* 2010; 117: 207–215.
7 Zeestraten EC, Benard A, Reimers MS, *et al*. The prognostic value of the apoptosis pathway in colorectal cancer: a review of the literature on biomarkers identified by immunohistochemistry. *Biomark Cancer* 2013; 5: 13–29.
8 Jiang X, Guo CX, Zeng XJ, *et al*. A soluble receptor for advanced glycation end-products inhibits myocardial apoptosis induced by ischemia/reperfusion via the JAK2/STAT3 pathway. *Apoptosis* 2015; 20: 1033–1047.
9 Xiao J, Sun B, Li M, *et al*. A novel adipocytokine visfatin protects against H(2)O(2)-induced myocardial apoptosis: a missing link between obesity and cardiovascular disease. *J Cell Physiol* 2013; 228: 495–501.
10 Naito AT, Okada S, Minamino T, *et al*. Promotion of CHIP-mediated p53 degradation protects the heart from ischemic injury. *Circ Res* 2010; 106: 1692–1702.
11 Zhang Y, Kohler K, Xu J, *et al*. Inhibition of p53 after acute myocardial infarction: reduction of apoptosis is counteracted by disturbed scar formation and cardiac rupture. *J Mol Cell Cardiol* 2011; 50: 471–478.
12 Mao Y, Wang X, Yan R, *et al*. Single point mutation in adeno-associated viral vectors-DJ capsid leads to improvement for gene delivery in vivo. *BMC Biotechnol* 2016; 16: 1.
13 Su Q, Li L, Zhou Y, *et al*. Induction of myocardial PDCD4 in coronary microembolization-related cardiac dysfunction: evidence from a large-animal study. *Cell Physiol Biochem* 2014; 34: 533–542.
14 Chen ZW, Qian JY, Ma JY, *et al*. TNF-alpha-induced cardiomyocyte apoptosis contributes to cardiac dysfunction after

coronary microembolization in mini-pigs. *J Cell Mol Med* 2014; 18: 1953–1963.
15 Gao CK, Liu H, Cui CJ, *et al*. Roles of MicroRNA-195 in cardiomyocyte apoptosis induced by myocardial ischemia-reperfusion injury. *J Genet* 2016; 95: 99–108.
16 Su H, Gorodny N, Gomez LF, *et al*. Noninvasive molecular imaging of apoptosis in a mouse model of anthracycline-induced cardiotoxicity. *Circ Cardiovasc Imaging* 2015; 8: e001952.
17 Su D, Guan L, Gao Q, *et al*. ROCK1/p53/NOXA signaling mediates cardiomyocyte apoptosis in response to high glucose in vitro and vivo. *Biochim Biophys Acta* 2017; 1863: 936–946.
18 Hong W, Tatsuo S, Shou-Dong W, *et al*. Resveratrol upregulates cardiac SDF-1 in mice with acute myocardial infarction through the deacetylation of cardiac p53. *PLoS One* 2015; 10: e0128978.
19 Nakamura H, Matoba S, Iwai-Kanai E, *et al*. p53 promotes cardiac dysfunction in diabetic mellitus caused by excessive mitochondrial respiration-mediated reactive oxygen species generation and lipid accumulation. *Circ Heart Fail* 2012; 5: 106–115.
20 Omori K, Kobayashi E, Komatsu H, *et al*. Involvement of a proapoptotic gene (BBC3) in islet injury mediated by cold preservation and rewarming. *Am J Physiol Endocrinol Metab* 2016; 310: e1016–e1026.
21 Rahimi A, Lee YY, Abdella H, *et al*. Role of p53 in cAMP/PKA pathway mediated apoptosis. *Apoptosis* 2013; 18: 1492–1499.
22 Han J, Flemington C, Houghton AB, *et al*. Expression of bbc3, a pro-apoptotic BH3-only gene, is regulated by diverse cell death and survival signals. *Proc Natl Acad Sci U S A* 2001; 98: 11318–11323.
23 Tu S, Liu ZQ, Fu JJ, *et al*. Inhibitory effect of p53 upregulated modulator of apoptosis targeting siRNA on hypoxia/reoxygenation-induced cardiomyocyte apoptosis in rats. *Cardiology* 2012; 122: 93–100.
24 Gao J, Zhang L, Wang WL, *et al*. Post-conditioning anti-PUMA treatment protects mice against mice heart I/R injury. *Eur Rev Med Pharmacol Sci* 2016; 20: 1623–1627.
25 Chen L, Knowlton AA. Mitochondria and heart failure: new insights into an energetic problem. *Minerva Cardioangiol* 2010; 58: 213–229.
26 Singh M, Dalal S, Singh K. Osteopontin: At the cross-roads of myocyte survival and myocardial function. *Life Sci* 2014; 118: 1–6.
27 Luo T, Liu H, Kim JK. Estrogen protects the female heart from ischemia/reperfusion injury through manganese superoxide dismutase phosphorylation by mitochondrial p38beta at threonine 79 and serine 106. *PLoS One* 2016; 11: e0167761.
28 Wang K, Yuan Y, Liu X, *et al*. Cardiac specific overexpression of mitochondrial Omi/HtrA2 induces myocardial apoptosis and cardiac dysfunction. *Sci Rep* 2016; 6: 37927.